Quantum Chemistry Based Force Field for Simulations of HMX

Grant D. Smith* and Rishikesh K. Bharadwaj

Department of Chemical and Fuels Engineering and Department of Materials Science and Engineering, University of Utah, Salt Lake City, Utah 84112

Received: December 3, 1998; In Final Form: February 24, 1999

The molecular geometries and conformational energies of octahydro-1,3,5,7-tetranitro-1,3,5,7-tetrazocine (HMX) and 1,3-dimethyl-1,3-dinitro methyldiamine (DDMD) and have been determined from high-level quantum chemistry calculations and have been used in parametrizing a classical potential function for simulations of HMX. Geometry optimizations for HMX and DDMD and rotational energy barrier searches for DDMD were performed at the B3LYP/6-311G** level, with subsequent single-point energy calculations at the MP2/6-311G** level. Four unique low-energy conformers were found for HMX, two whose conformational geometries correspond closely to those found in HMX polymorphs from crystallographic studies and two additional, lower energy conformers that are not seen in the crystalline phases. For DDMD, three unique low-energy conformers, and the rotational energy barriers between them, were located. In parametrizing the classical potential function for HMX, nonbonded repulsion/dispersion parameters, valence parameters, and parameters describing nitro group rotation and out-of-plane distortion at the amine nitrogen were taken from our previous studies of dimethylnitramine. Polar effects in HMX and DDMD were represented by sets of partial atomic charges that reproduce the electrostatic potential and dipole moments for the low-energy conformers of these molecules as determined from the quantum chemistry wave functions. Parameters describing conformational energetics for the C−N−C−N dihedrals were determined by fitting the classical potential function to reproduce relative conformational energies in HMX as found from quantum chemistry. The resulting potential was found to give a good representation of the conformer geometries and relative conformer energies in HMX and a reasonable description of the low-energy conformers and rotational energy barriers in DDMD.

I. Introduction

In previous work[1] we presented a classical potential function for dimethylnitramine (DMNA; see Figure 1) based on high-level quantum chemistry calculations of molecular geometries and conformational energies. In that work, a systematic study of the influence of basis set and electron correlation on molecular geometries, nitro group rotational energies, and inversion energies about the amine nitrogen was performed. Nitro group rotation and inversion are the important modes of molecular flexibility in DMNA, as illustrated in Figure 1. It was found that while the barrier for rotation of the nitro group is large (around 10 kcal/mol), the C_{2v} inversion barrier between the pyramidal (at the amine nitrogen) C_s ground states is less than 1 kcal/mol. The force field, parametrized to reproduce the quantum chemistry geometries and energies for DMNA, was shown to accurately reproduce these data. Gas-phase molecular dynamics simulations using the quantum chemistry based force field accurately reproduced the gas-phase structure of DMNA as determined from electron diffraction studies. Liquid-phase molecular dynamics simulations yielded thermophysical and transport properties of DMNA in good agreement with available experimental data.[1,2]

In this work we extend our studies of nitramine compounds to include octoahydro-1,3,5,7-tetranitro-1,3,5,7-tetrazocine (HMX) and 1,3-dimethyl-1,3-dinitro methyldiamine (DDMD). These compounds are illustrated in Figures 2 and 3, respectively. Our intention is to parametrize a classical force field for HMX that accurately reproduces the conformational geometries and energetics for this flexible molecule.[3] Previous potential functions for HMX[4,5] have considered rigid molecules and hence have been concerned only with the intermolecular potential. While it is reasonable to assume that the rigid molecule approach may be useful in predicting some static properties of crystalline HMX, we believe that a reasonable representation of conformational flexibility is required in order to accurately predict liquid-phase thermophysical and transport properties from molecular dynamics simulations and may be important in determining dynamic properties of crystalline HMX and even static properties near phase transitions.

II. Conformations of HMX

HMX is a conformationally flexible cyclic molecule that in its four crystalline polymorphs, labeled α through δ, exists in one of two primary conformations. In the α form,[6] the HMX molecule has C_2 symmetry as illustrated in Figure 2. In the γ and δ forms[7,8] the conformations of HMX are quite similar to that found in the α form but without precise 2-fold axial symmetry. The molecular conformation of HMX in the β form[9] is quite different from that in the other phases, as illustrated in Figure 2. Here, the molecule has C_i symmetry. It is also possible that other low-energy conformations of HMX exist in the amorphous phases (gas and liquid), where the restrictions imposed by regular crystalline packing are removed.

To investigate the relative conformational energies in HMX, we have performed high-level quantum chemistry geometry

* To whom correspondence should be addressed.

10.1021/jp984599p CCC: $18.00
Published on Web 04/21/1999

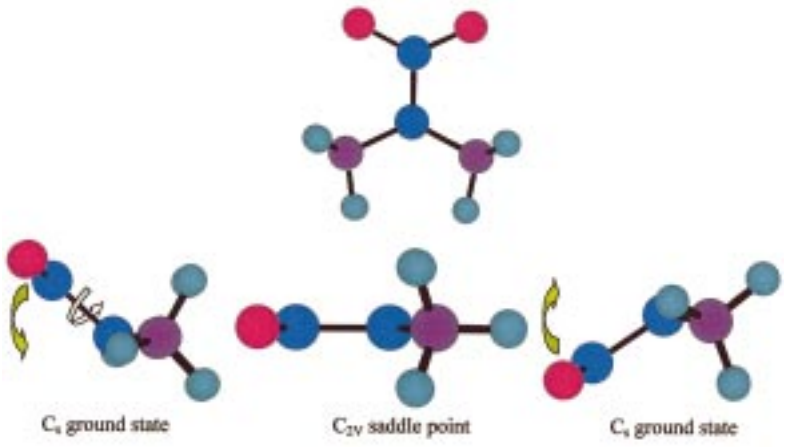

Figure 1. Pyramidal ground-state (C_s) and planar saddle-point geometry (C_{2v}) for DMNA. Arrows denote conformational flexibility due to nitro group rotation and inversion (out-of-plane bending) at the amine nitrogen. O = red, N = blue, C = mauve.

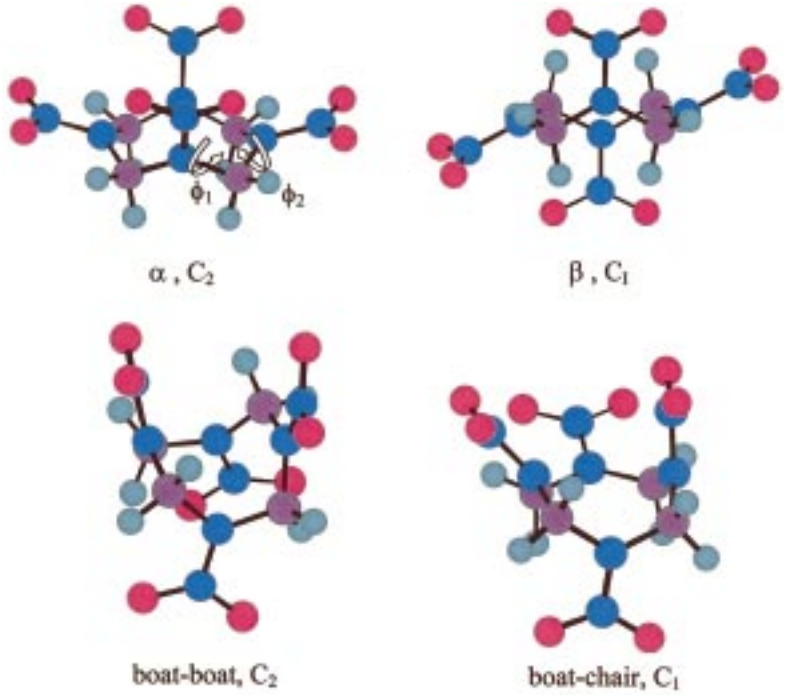

Figure 2. B3LYP/6-311G** geometries of the low-energy HMX conformers. The arrows denote a representative methylene-centered dihedral pair corresponding to the dihedrals in DDMD (see text). O = red, N = blue, C = mauve.

optimizations and single-point energy calculations on single HMX molecules. We believe that a classical force field, parametrized to reproduce the conformational energies and rotational energy barriers for a single (gas-phase) HMX molecule, will, given an accurate description of intermolecular interactions, correctly reproduce conformations and conformational dynamics in the liquid and crystalline phases. On the basis of our studies of nitramide and DMNA, we performed geometry optimizations using density functional theory at the B3LYP[10]/6-311G** level and subsequent ab initio single-point energy calculations at the MP2/6-311G** level, which includes an estimate of electron correlation effects using second-order Møller−Plesset (MP2) perturbation theory.[11,12] Yoshida and Matsuura have recently demonstrated the greater accuracy of conformational energies obtained from MP2 ab initio calculations compared to density functional theory (DFT) calculations.[13] Reference 13 is a comprehensive comparison of the conformational energies of 1,2-dimethoxyethane (DME) determined using various density function methods with MP2 ab initio methods. The accuracy of the MP2 conformational energies for DME has been thoroughly established through extensive comparisons of populations with gas phase, matrix-isolation, liquid phase and aqueous solution experimental data.[14−21] While the conformational energies for DME were found to be better predicted by DFT methods using the B3 exchange functional than other functionals, important differences between DFT and MP2 conformational energies were found. In addition, we have found that while the energy of the tgt conformer of DME relative to the ttt is reduced at the MP2 level by inclusion of additional polarization functions beyond DZP, this reduction, required to bring the DME conformational populations in agreement with experimental results, is much smaller using DFT methods. Because of the large size of the HMX molecules, previously published electronic structure calculations have been limited to a much lower level of theory and have not involved geometry optimizations, instead using the crystallographic molecular geometries.[22−25]

The low-energy conformers of HMX determined at the B3LYP/6-311G** level are illustrated in Figure 2, and the ring dihedral angles and out-of-plane bending angles at the amine

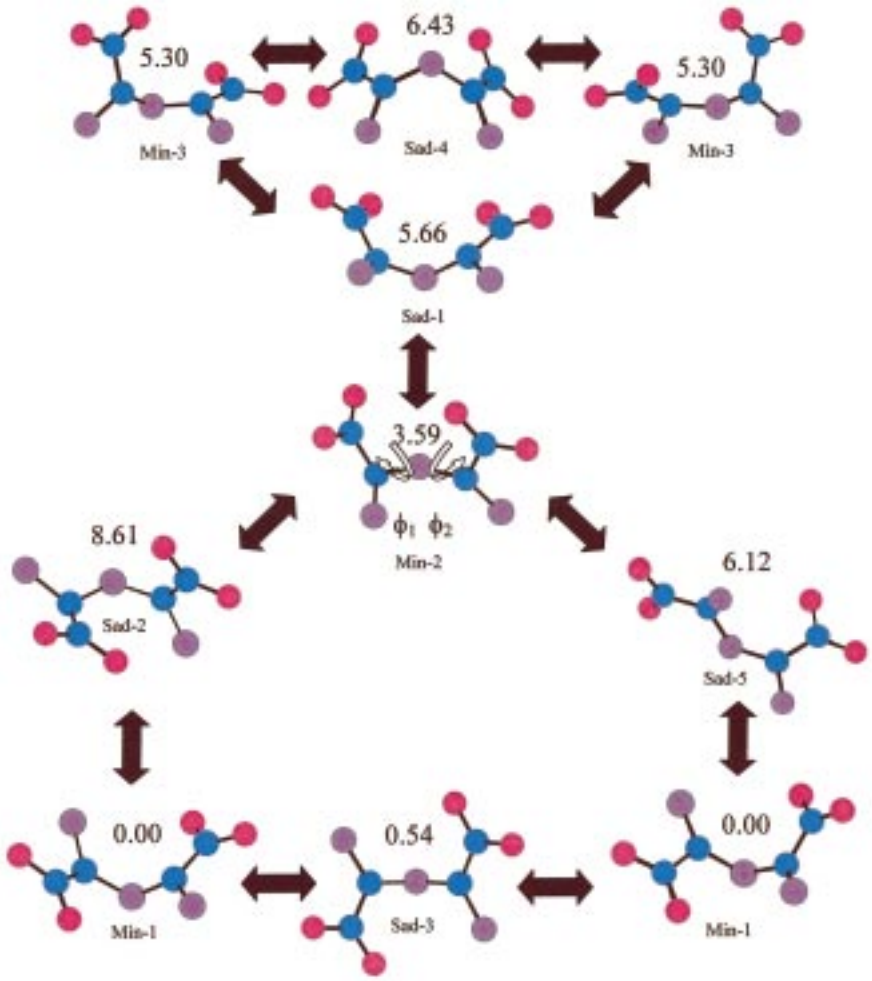

Figure 3. B3LYP/6-311G** geometries of DDMD (Min-1 to Min-3) and the rotational energy barriers between them (Sad-1 to Sad-5). Relative energies in kcal/mol, determined at the MP2/6-311G** level, are indicated. The C−N−C−N dihedrals ϕ_1 and ϕ_2 are denoted. O = red, N = blue, C = mauve.

TABLE 1: HMX Conformer Energies and Geometries

			ring dihedral angles (deg)								out-of-plane angles (deg)			
conformer	source	energy kcal/mol	ϕ_1	ϕ_2	ϕ_3	ϕ_4	ϕ_5	ϕ_6	ϕ_7	ϕ_8	δ_1	δ_2	δ_3	δ_4
α	exp[a]	*b*	−105.5	99.4	−63.8	69.5	−105.0	100.7	−64.7	68.2	12.3	3.6	13.4	3.2
α	qc[c]	4.3 (2.9)	−94.9	94.9	−70.3	70.3	−94.9	94.9	−70.3	70.3	19.2	4.1	19.2	4.1
α	ff[d]	3.2	−98.6	109.1	−69.4	61.9	−97.6	96.2	−58.0	58.3	17.9	9.4	7.2	1.2
β	exp[e]	- - -	−18.1	−43.4	117.1	−101.6	18.1	43.4	−117.2	101.7	8.5	21.3	8.5	21.3
β	qc[c]	0.8 (0.8)	−20.6	−41.9	113.8	−100.9	20.6	41.9	−113.8	100.9	7.5	19.4	7.5	19.4
β	ff[d]	0.6	−23.6	−48.9	116.7	−85.2	2.3	57.5	−102.0	92.0	4.1	18.2	2.1	5.7
BC	qc[c]	0.0 (0.0)	63.6	−55.7	96.3	−56.3	−61.2	73.3	36.1	−98.5	21.5	1.8	18.5	14.0
BC	ff[d]	0.0	58.1	−59.2	106.8	−59.4	−54.3	64.2	44.8	−100.2	8.1	2.5	5.8	18.0
BB	qc[c]	0.5 (1.4)	−26.4	73.3	26.4	−73.3	−26.4	73.3	26.4	−73.3	10.0	10.0	10.0	10.0
BB	ff[d]	−0.6	−40.5	71.4	36.6	−73.3	−32.3	67.6	36.5	−65.9	14.7	11.6	0.9	0.1

[a] Reference 6. [b] Single molecule energies are not available. [c] Quantum chemistry MP2(B3LYP) energies. [d] Force field energies. [e] Reference 9.

nitrogen are tabulated in Table 1. The relative conformer energies, determined at the B3LYP/6-311G**//MP2/6-311G** geometry/energy level, are also tabulated in Table 1. All quantum chemistry calculations were performed using the quantum chemistry packages GAUSSIAN 94[26] and GAUSSIAN 98[27] on DEC Alpha workstations and in parallel on the SGI Origin 2000 system and the IBM SP2 at the Center for High Performance Computing at the University of Utah. The "α" conformer, with C_2 symmetry, corresponds to the geometry found in the α polymorph of crystalline HMX and is quite similar to the HMX conformations in the γ and δ forms, while the "β" conformer, with C_i symmetry, corresponds to the HMX geometry found in the β form. In addition to these conformations, we found two low-energy conformations of HMX not seen in the crystalline phases. The global minimum boat-chair (BC) conformer has C_1 symmetry, while the boat-boat (BB) conformer has C_2 symmetry. Comparison of the ring conformations and out-of-plane bending angles for the α and β conformers obtained from B3LYP/6-311G** optimization with experimentally determined geometries for the molecules in the respective crystalline polymorphs reveals good agreement, as shown in Table 1. This agreement supports our supposition that the B3LYP/6-311G** level of theory is adequate for geometry optimizations in nitramine compounds. The agreement also

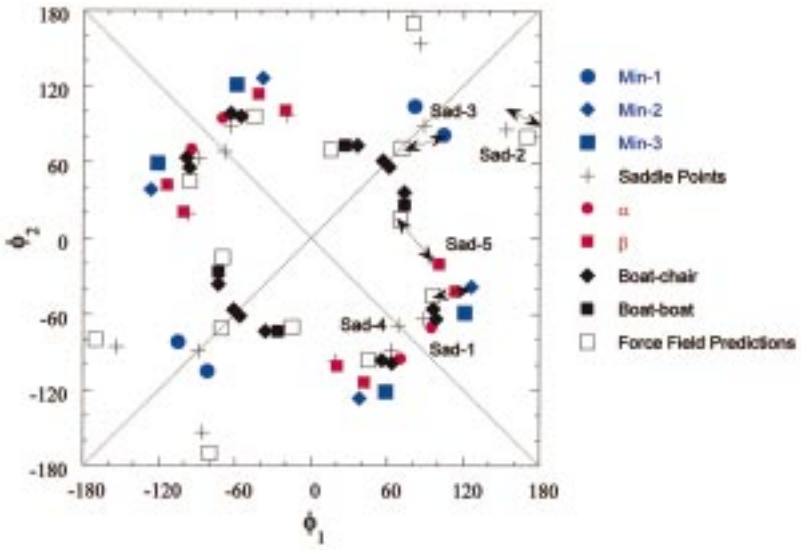

Figure 4. Dihedral geometry of the low-energy conformers of DDMD and the rotational energy barriers between them. Also shown are the geometries for methylene-centered dihedral pairs in the low-energy conformers of HMX. DDMD conformers and rotational energy barriers from the classical force field are also shown, with arrows connecting them with corresponding ab initio geometries.

indicates that the molecular geometries of HMX in the crystalline polymorphs are not greatly distorted from the optimized gas-phase geometries, i.e., that condensed-phase effects in the crystalline phase do not strongly perturb the conformational geometry of HMX. However, the fact that the lowest energy gas-phase conformers (BB and BC) are not found in the crystalline phases indicates that intermolecular interactions are important in determining the conformations of molecules in the stable crystalline structures.

III. Conformations of DDMD

In developing a classical potential for the conformational flexible HMX molecule, we begin with the assumption that the dispersion/repulsion and valence parameters, which we employed successfully in our description of DMNA, are transferable to other nitramine compounds such as HMX. Hence, to complete the potential for HMX, we must determine the partial atomic charges that best describe polar interactions and valence parameters for the N−C−N bend and C−N−C−N (or N−C−N−C) torsions, interactions that do not occur in DMNA. The torsional potential strongly influences the librational flexibility of the HMX ring structure and the ease with which conformational isomerization can occur. DDMD, illustrated in Figure 3, is the ideal model compound for studying the rotational energetics of the C−N−C−N dihedrals that form the cyclic structure of HMX; both the conformer energies and geometries as well as the energies and geometries of the rotational energy barriers can be more readily determined from quantum chemistry for this smaller molecule than for the computationally demanding HMX molecule. In this section we consider the conformational energetics of DDMD and in the following section parametrize a force field for HMX and DDMD and finally compare predictions with quantum chemistry results.

The low-energy conformers and saddle points (rotational energy barriers) for DDMD are summarized in Table 2 and are illustrated in Figure 3. Figure 4 is a plot of ϕ_2 vs ϕ_1 for the C−N−C−N−C dihedral pairs (denoted in Figure 3) for the DDMD conformers and rotational energy barriers as well as for the α, β, BC, and BB conformers of HMX (denoted in Figure 2) obtained at the B3LYP/6-311G** level. It can be seen that dihedral pair conformations similar to the lowest energy DDMD conformer (Min-1) are found only in the lowest energy HMX conformers, BC and BB. These conformations are not seen in crystalline HMX (see above discussion). Conformations resembling those found in the higher energy DDMD minima (Min-2 and Min-3) are found in each of the HMX conformers except the BB. Table 2 shows the energy of DDMD constrained to the conformation (as determined from quantum chemistry) of representative torsional pairs in both α- and β-HMX. The resulting DDMD energies are quite similar to those of the Min-2 and Min-3 conformers of DDMD.

TABLE 2: Conformers and Rotational Energy Barriers for DDMD

	B3LYP/6-311G** geometry		energy (kcal/mol)	
conformer	ϕ_1	ϕ_2	BL3YP/ 6-311G**	MP2/ 6-311G**
Min-1	81.5 (70)[a]	104.3 (70)	0.00	0.00 (0.0)
Min-2	38.2 (45)	−126.5 (−96)	4.82	3.59 (2.9)
Min-3	58.9	−121.3	5.49	5.30
Sad-1	63.5	−88.5	6.28	5.66
Sad-2	85.7 (80)	153.6 (170)	9.46	8.61 (7.5)
Sad-3	88.9	88.9		0.54
Sad-4	68.6	−68.6	6.35	6.43
Sad-5	19.5 (−15)	−97.1 (−70)	6.06	6.12 (3.5)
α[b]	70.3	−94.86	5.68	5.51 (2.9)[c]
β[b]	113.8	−41.6	4.96	4.25 (3.3)[c]

[a] Numbers in parentheses are from force field calculations. [b] Typical angles for a methylene-centered dihedral pair for the respective HMX conformer from quantum chemistry geometries. [c] Dihedral angles were constrained to the quantum chemistry values.

Examination of Figure 4 reveals that conformations of the C−N−C−N dihedrals in the low-energy conformers of DDMD and HMX are restricted to $|\phi| \leq 120°$. The trans conformation of the C−N−C−N dihedral leads to strong steric interference between a nitro oxygen atom and the amine nitrogen of the neighboring nitramine group. This interaction can be only partially relieved by out-of-plane distortion of the nitro group. Complete relief of the interaction would require significant rotation of the nitro group, which is energetically unfavorable. A consequence of the nitro oxygen−amine nitrogen steric interaction is that the barrier for rotation from Min-1 to Min-2 is significantly higher through Sad-2 than through Sad-5 (see Figure 3 and Table 2). It can also be seen that all methylene-

TABLE 3: Partial Atomic Charges for HMX and DDMD

atom	DDMD	HMX	DDMD[a]
C	−0.4166		
C (methylene)		−0.4320	−0.4320
C (methyl)			−0.6480
N (amine)	0.1598	0.0451	0.0451
N (nitro)	0.5601	0.6881	0.6885
O	−0.3599	−0.3668	−0.3668
H	0.1562	0.2160	0.2160

[a] Using HMX charges; see text.

TABLE 4: Dipole Moments of HMX and DDMD Conformers

	molecular dipole moment (D)	
conformer	MP2/6-311G**	force field
DDMD Min-1	2.17	1.76
DDMD Min-2	6.41	6.77
DDMD Min-3	6.13	6.25
HMX α	8.41	8.78
HMX β	0.0	0.0
HMX BC	5.45	5.45

centered dihedral pairs in the HMX conformers lie closer to the cis−cis origin of Figure 4 than in the low-energy conformers of DDMD. This is a consequence of conformational restrictions in the cyclic HMX molecule. However, the similarity between the energies obtained for the DDMD conformers constrained to α- and β-HMX dihedral angles and the fully relaxed Min-2 and Min-3 DDMD conformers indicates that the ring conformations of α- and β-HMX are not highly strained relative to the latter DDMD conformers. It should be remembered that the Min-2 and Min-3 conformers of DDMD are already significantly higher in energy than the global Min-1 conformer.

IV. Force Field Parametrization

Partial Atomic Charges. Partial atomic charges were determined for each of the low-energy DDMD conformers and for the α, β, and BC conformers of HMX according to the following algorithm. The electrostatic potential at a grid of 30000−70000 points (depending upon the compound) lying within 4 Å of any atom but excluding points within the van der Waals radius of any atom was determined for each conformer from the MP2 wave functions. The set of partial atomic charges that best reproduced the electrostatic potential at the grid points, and the molecular dipole moment, was determined with the constraints that "like" atoms had equal charges. The charges, which were quite similar for each conformer, were averaged to obtain the average charges shown in Table 3. As can be seen in Table 4, the charges do a good job in reproducing the molecular dipole moments of each conformer, indicating that the charges are not strongly conformation-dependent. The charges for DDMD are quite similar to those for HMX. For the purpose of investigating the accuracy of the potential function for DDMD and for optimizing the transferability of the potential function, the HMX charges were used in describing DDMD, with the methyl carbon charge set to be equal to the methylene carbon charge minus a hydrogen charge. These charges are also given in Table 3. In practice, the conformational energies of DDMD were found to depend little on which set of DDMD charges was employed.

Torsional Potential Function. We employed the same valence potential function for HMX and DDMD as derived for DMNA.[1] This potential function, along with the nonbonded parameters used,[1] is summarized in Table 5. Nonbonded interactions (Coulomb and dispersion/repulsion) are considered intramolecularly for all atoms separated by three or more bonds and for all intermolecular interatomic interactions. The only additional potential parameters required to complete the description of HMX and DDMD are the bending parameters for the N−C−N bend and the torsional parameters for rotations about the C−N−C−N (or N−C−N−C) dihedrals. The former parameters were determined from the quantum chemistry geometry and force constants for DDMD. The latter parameters were determined by obtaining the best representation of the quantum chemistry conformer energies and geometries for the α, β, BB, and BC conformers of HMX while at the same time maintaining a reasonable description of the conformational energies and rotational energy barriers in DDMD.

TABLE 5: Force Field for HMX and DDMD

Bond Stretches, $U = {}^1/_2 k^s_{ij}(r_{ij} - r^o_{ij})^2$

stretch	k^s_{ij} (kcal mol^{-1} Å^{-2})	r^o_{ij} (Å)
O−N	1990.1	1.23
N−N	991.7	1.36
N−C	672.1	1.44
C−H	641.6	1.09

Valence Bends, $U = {}^1/_2 k^b_{ijk}(\theta_{ijk} - \theta^o_{ijk})^2$

bend	k^b_{ijk} (kcal mol^{-1} rad^{-2})	θ^o_{ijk} (rad)
O−N−O	125.0	2.1104
O−N−N	125.0	1.8754
N−N−C	130.0	1.6723
C−N−C	70.0	1.8430
N−C−H	86.4	1.8676
H−C−H	77.0	1.8938
N−C−N	70.0	1.9289

Torsions, $U = {}^1/_2 k^t_{ijkl}[1 - \cos(n\phi_{ijkl})]$

torsion	k^t_{ijkl} (kcal mol^{-1})	n
O−N−N−C	8.45	2
O−N−N−C	0.79	4
O−N−N−C	0.004	8
H−C−N−C[a]	−0.16	3
C−N−C−N	3.30	1
C−N−C−N	−1.61	2
C−N−C−N	0.11	3

Out-of-plane Bends, $U = {}^1/_2 k^d_{ijkl}\delta_{ijkl}^2$

out-of-plane bend	k^d_{ijkl} (kcal mol^{-1} rad^{-2})
C−N−C-*N	8.0[b]
O−N−O-*N	89.3

Nonbonded, $U = A_{ij}\exp(-B_{ij}r_{ij}) - C_{ij}/r_{ij}^6$

atoms	A_{ij} (kcal mol^{-1})	B_{ij} (Å^{-1})	C_{ij} (kcal mol^{-1} Å^6)
C···C	14976.0	3.090	640.8
H···H	2649.7	3.740	27.4
C···H	4320.0	3.415	138.2
N···N	60833.9	3.780	500.0
O···O	75844.8	4.063	398.9

[a] This interaction replaces the H−C−N−N torsion in the DMNA force field. Addition of a C−N−C−*N out-of-plane bending function with a force constant of 4.0 kcal mol^{-1} rad^{-2} yields the same inversion barrier in DMNA as the previously published potential. [b] A value of 4.0 kcal mol^{-1} rad^{-2} was used for DDMD. A slightly stiffer potential was found to yield somewhat improved conformational geometries for HMX.

V. Comparison of Force Field and Quantum Chemistry

The force field energies and geometries for the low-energy conformers of HMX are given in Table 1. The force field does

a credible job in reproducing the quantum chemistry conformational energies and geometries for HMX. Relative to the global minimum BC conformer, the force field accurately reproduces the energy of the β conformer while yielding an energy for the α conformer that lies between the MP2 and B3LYP values. In contrast to quantum chemistry, the force field yields an energy for the BB conformer that is lower than that of the boat-chair. For future application of the force field to crystalline HMX it is important that the difference in energy between the α and β conformers be well represented. According to our quantum chemistry calculations, this difference is 3.5 ± 1.0[28] kcal/mol at the MP2 level and 2.1 kcal/mol at the B3LYP level, while the force field yields 2.6 kcal/mol. If the ring dihedrals are constrained to the quantum chemistry values, the force field yields (relative to a fully relaxed BC conformation) 4.9 and 1.6 kcal/mol, respectively, for the α and β conformers, with a corresponding energy difference of 3.3 kcal/mol.

The conformer energies and geometries for DDMD from the force field are given in Table 2 and illustrated in Figure 4. The force field does a reasonable job in representing the geometries and energies of the Min-1 and Min-2 conformers as well as the high-energy saddle point Sad-2. Min-1 is found to be a single minimum with C_2 symmetry as opposed to split minima separated by a low-energy saddle point as predicted by quantum chemistry. No conformer corresponding to Min-3 exists on the DDMD conformational energy surface. The low-energy saddle point (Sad-5) separating Min-1 and Min-2 is not as well represented by the force field, lying only 0.7 kcal/mol above the energy of Min-2 as opposed to 2.5 and 1.2 kcal/mol predicted by quantum chemistry at the MP2 and B3LYP levels, respectively.

Acknowledgment. This research is funded in part by the University of Utah Center for the Simulation of Accidental Fires and Explosions (C-SAFE), funded by the Department of Energy, Lawrence Livermore National Laboratory, under Subcontract B341493. An allocation of computer time from the Center for High Performance Computing at the University of Utah is gratefully acknowledged. CHPC's IBM SP2 is funded in part by NSF Grant CDA9601580 and IBM's SUR grant to the University of Utah. CHPC's SGI Origin 2000 system is funded in part by the SGI Supercomputing Visualization Center Grant.

References and Notes

(1) Smith, G. D.; Bharadwaj, R. K.; Bedrov, D.; Ayyagari, C. *J. Phys. Chem. B* **1999**, *103*, 705.

(2) Smith, G. D.; Bedrov, D. In preparation.

(3) The potential for HMX presented in this work is parametrized to reproduce conformational geometries and energies of HMX and DDMD and hence the molecular flexibility required for accurate simulations of liquid-phase properties. The ability of the flexible HMX potential to accurately represent HMX polymorphs must yet be determined. The simple diagonal (no valence cross-terms) representation of bonded interactions is not expected to yield an accurate description of vibrational frequencies.

(4) Sorescu, D. C.; Rice, B. M.; Thompson, D. L. *J. Phys. Chem. B* **1998**, *102*, 6692.

(5) Sewell, T. D. *AIP Conf. Proc.* **1998**, *429*, 269.

(6) Cady, H. H.; Larson, A. C.; Cromer, D. T. *Acta Crystallogr*. **1963**, *16*, 617.

(7) Main, P.; Cobbledick, R. E.; Small, R. W. H. *Acta Crystallogr*. **1985**, *C41*, 1351.

(8) Cobbledick, R. E.; Small, R. W. H. *Acta Crystallogr*. **1974**, *B30*, 1918.

(9) Choi, C. S.; Boutin, H. P. *Acta Crystallogr*. **1970**, *B26*, 1235.

(10) Becke, A. D. *J. Chem. Phys.* **1993**, *93*, 5648.

(11) Møller, C.; Plesset, M. S. *Phys. Rev.* **1934**, *46*, 618.

(12) Binkley, J. S.; Pople, J. A. *Int. J. Quantum Chem.* **1975**, *9*, 229.

(13) Yoshida, H.; Matsuura, H. *J. Phys. Chem. A* **1998**, *102*, 2691.

(14) Jaffe, R. L.; Smith, G. D.; Yoon, D. Y. *J. Phys. Chem.* **1993**, *97*, 12745.

(15) Smith, G. D.; Jaffe, R. L.; Yoon, D. Y. *J. Phys. Chem.* **1993**, *97*, 12752.

(16) Smith, G. D.; Jaffe, R. L.; Yoon, D. Y. *J. Am. Chem. Soc.* **1995**, *117*, 530.

(17) Bedrov, D.; Pekny, M.; Smith, G. D. *J. Phys. Chem. B* **1998**, *102*, 996.

(18) Bedrov, D.; Borodin, O.; Smith, G. D. *J. Phys. Chem. B* **1998**, *102*, 5683.

(19) Bedrov, D.; Smith, G. D. *J. Phys. Chem. B* **1998**, *102*, 9565.

(20) Bedrov, D.; Smith, G. D. *J. Chem. Phys.* **1998**, *109*, 8118.

(21) Yoshida, H.; Tanaka, T.; Matsuura, H. *Chem. Lett.* **1996**, 637.

(22) Kohno, Y.; Maekawa, K.; Azuma, N.; Tsuchioka, T.; Hashizume, T.; Imanura, A. *Kogyo Kayaku* **1992**, *53*, 227.

(23) Kohno, Y.; Maekawa, K.; Tsuchioka, T.; Hashizume, T.; Imamura, A. *Chem. Phys. Lett.* **1993**, *214*, 603.

(24) Kohno, Y.; Maekawa, K.; Tsuchioka, T.; Hashizume, T.; Imamura, A. *Combust. Flame* **1994**, *96*, 343.

(25) Pati, R.; Sahoo, N.; Das, T. P.; Ray, S. N. *J. Phys. Chem. A* **1997**, *101*, 8302.

(26) Frisch, M. J.; Trucks, G. W.; Schlegel, H. B.; Gill, P. M. W.; Johnson, B. G.; Robb, M. A.; Cheeseman, J. R.; Keith, T.; Petersson, G. A.; Montgomery, J. A.; Raghavachari, K.; Al-Laham, M. A.; Zakrzewski, V. G.; Ortiz, J. V.; Foresman, J. B.; Cioslowski, J.; Stefanov, B. B.; Nanayakkara, A.; Challacombe, M.; Peng, C. Y.; Ayala, P. Y.; Chen, W.; Wong, M. W.; Andres, J. L.; Replogle, E. S.; Gomperts, R.; Martin, R. L.; Fox, D. J.; Binkley, J. S.; Defrees, D. J.; Baker, J.; Stewart, J. P.; Head-Gordon, M.; Gonzalez, C.; Pople, J. A. *Gaussian 94*, revision D.1; Gaussian, Inc.: Pittsburgh, PA, 1995.

(27) Frisch, M. J.; Trucks, G. W.; Schlegel, H. B.; Scuseria, G. E.; Robb, M. A.; Cheeseman, J. R.; Zakrzewski, V. G.; Montgomery, J. A., Jr.; Stratmann, R. E.; Burant, J. C.; Dapprich, S.; Millam, J. M.; Daniels, A. D.; Kudin, K. N.; Strain, M. C.; Farkas, O.; Tomasi, J.; Barone, V.; Cossi, M.; Cammi, R.; Mennucci, B.; Pomelli, C.; Adamo, C.; Clifford, S.; Ochterski, J.; Petersson, G. A.; Ayala, J. Y.; Cui, Q.; Morokuma, K.; Malick, D. K.; Rabuck, A. D.; Raghavachari, K.; Foresman, J. B.; Cioslowski, J.; Ortiz, J. V.; Stefanov, B. B.; Liu, G.; Liashenko, A.; Piskorz, P.; Komaromi, I.; Gomperts, R.; Martin, R. L.; Fox, D. J.; Keith, T.; Al-Laham, M. A.; Peng, C. Y.; Nanayakkara, A.; Gonzalez, C.; Challacombe, M.; Gill, P. M. W.; Johnson, B.; Chen, A.; Wong, M. W.; Andres, J. L.; Gonzalez, C.; Head-Gordon, M.; Replogle, E. S.; Pople, J. A. *Gaussian 98*, Revision A.1; Gaussian, Inc.: Pittsburgh, PA, 1998.

(28) On the basis of the basis set dependence of conformational energies in nitramide and DMNA, we estimate the uncertainties in the conformational energies of HMX from the B3LYP/6-311G**//MP2/6-311G** quantum chemistry calculations to be around 1 kcal/mol.